

REPORT DOCUMENTATION PAGE

Form Approved
OMB No. 0704-0188

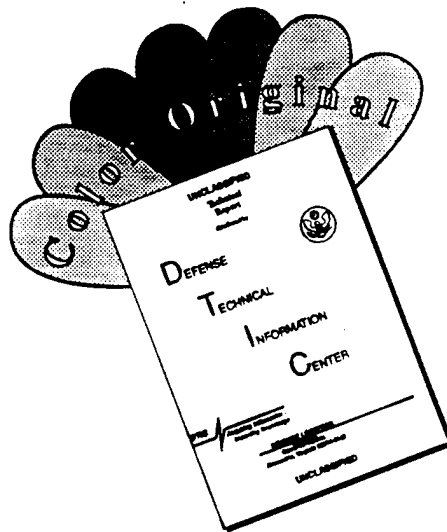
Public reporting burden for this collection of information is estimated to average 1 hour per response, including the time for reviewing instructions, searching existing data sources, gathering and maintaining the data needed, and completing and reviewing the collection of information. Send comments regarding this burden estimate or any other aspect of this collection of information, including suggestions for reducing this burden, to Washington Headquarters Services, Directorate for Information Operations and Reports, 1215 Jefferson Davis Highway, Suite 1204, Arlington, VA 22202-4302, and to the Office of Management and Budget, Paperwork Reduction Project (0704-0188), Washington, DC 20503.

1. AGENCY USE ONLY (Leave blank)	2. REPORT DATE	3. REPORT TYPE AND DATES COVERED	
	Feb. 13, 1996	Final 95 Aug 01 - 96 Feb 13	
4. TITLE AND SUBTITLE		5. FUNDING NUMBERS	
High Temperature Heterojunction Transistors with High Gain and Wide Bandwidth		Contract F49620-95-C-0061 65502F 3005/SS	
6. AUTHOR(S)		8. PERFORMING ORGANIZATION NAME(S) AND ADDRESS(ES)	
H. Paul Maruska		AFOSR-TR-96 0124	
7. PERFORMING ORGANIZATION NAME(S) AND ADDRESS(ES)		9. SPONSORING/MONITORING AGENCY NAME(S) AND ADDRESS(ES)	
NZ Applied Technologies 150 C New Boston Street Woburn, MA 01801		Air Force Office of Scientific Research - NE Bolling AFB DC 20332-0001	
11. SUPPLEMENTARY NOTES		10. SPONSORING/MONITORING AGENCY REPORT NUMBER	
12a. DISTRIBUTION/AVAILABILITY STATEMENT		12b. DISTRIBUTION CODE	
See DOD 5230.24 "Distribution Statements on Technical Documents"		DISTRIBUTION STATEMENT A Approved for public release; Distribution Unlimited 19960320 082	
13. ABSTRACT (Maximum 200 words)		NZ Applied Technologies has successfully grown the world's first single crystal thin films of $Zn_{0.5}Ge_{0.5}N$. There is no evidence that any other investigators have ever produced single crystal films of this ternary nitride material before us. The growth temperature must be at least 650° C in our plasma-enhanced MOCVD system to deposit films of $Zn_{0.5}Ge_{0.5}N$ with excellent crystal quality. Strong x-ray single crystal diffraction spectra have been obtained for films grown on (0001) sapphire substrates and sapphire pre-coated with GaN, and films had the c-axis perpendicular to the substrate surface. A reflection high energy electron diffraction study has confirmed the $Zn_{0.5}Ge_{0.5}N$ crystallinity. $Zn_{0.5}Ge_{0.5}N$ possesses the same wurtzite lattice as GaN, and has lattice parameters $a = 3.1826\text{\AA}$ and $c = 5.2132\text{\AA}$; differing from GaN by only 0.2 %. The bandgap of $Zn_{0.5}Ge_{0.5}N$ is 2.8 eV, giving band-to-band optical transitions at 442 nm in the deep blue region of the spectrum, which should lead to the production of a new class of bright blue light-emitting and laser diodes. The c/a ratio for $Zn_{0.5}Ge_{0.5}N$ is 1.638, indicating a rhombohedral lattice expansion, suggesting important nonlinear optical properties for this new material. Thus the development of high performance modulation-doped-field-effect-transistors (MODFETs) and heterojunction-bipolar-transistors (HBTs) can be expected.	
14. SUBJECT TERMS		15. NUMBER OF PAGES	
Ternary nitride semiconductors Metalorganic chemical vapor deposition Single crystal epitaxial films		29	
16. PRICE CODE			
17. SECURITY CLASSIFICATION OF REPORT	18. SECURITY CLASSIFICATION OF THIS PAGE	19. SECURITY CLASSIFICATION OF ABSTRACT	20. LIMITATION OF ABSTRACT
N/A	N/A	N/A	SAR

NSN 7540-01-280-5500

Standard Form 298 (Rev. 2-89)
Prescribed by ANSI Std Z39-18
298-102

DISCLAIMER NOTICE



THIS DOCUMENT IS BEST
QUALITY AVAILABLE. THE COPY
FURNISHED TO DTIC CONTAINED
A SIGNIFICANT NUMBER OF
COLOR PAGES WHICH DO NOT
REPRODUCE LEGIBLY ON BLACK
AND WHITE MICROFICHE.

FINAL TECHNICAL REPORT

February 13, 1996

Contract F49620-95-C-0061

High Temperature Heterojunction Transistors with High Gain and Wide Bandwidth

NZ Applied Technologies
150-C New Boston Road
Woburn, MA 01801
(617) 935-2030

H. Paul Maruska

Distribution Notice to be selected by Contract Monitor

AIR FORCE OFFICE OF SCIENTIFIC RESEARCH
BOLLING AIR FORCE BASE, DC 20332-0001

SBIR Rights Notice (June 1987)

These SBIR Data are furnished with SBIR rights under Contract No. F49620-95-C-0061. For a period of four years after acceptance of all items to be delivered under this contract, the Government agrees to use these data for Government purposes only and they shall not be disclosed outside the Government (including disclosure for procurement purposes) during such period without permission of the grantee, except that, subject to the foregoing use and disclosure prohibitions, such data may be disclosed for use by support contractors. After the aforesaid 4-year period, the Government has a royalty-free license to use, and to authorize others to use on its behalf, these data for Government purposes, but is relieved of all disclosure prohibitions and assumes no liability for unauthorized use of these data by third parties. This notice shall be affixed to any reproductions of these data in whole or in part.

The above referenced SBIR Data is located on pages 3 to 26 of this document.

Abstract

NZ Applied Technologies has developed the first set of materials deposition conditions for creating epitaxial thin films of the stoichiometric ternary nitride compound $Zn_{0.5}Ge_{0.5}N$, a new wide bandgap material appropriate for introduction into a wide variety of electronic and optoelectronic devices.

Applications include blue light-emitting diodes, blue laser diodes, heterostructure transistors for high temperature operation, dielectric mirrors for wavelength filtering, and cold cathodes for field emission displays and high performance microwave vacuum tubes. With a direct bandgap in the blue region of the spectrum, $Zn_{0.5}Ge_{0.5}N$ can simply be used to fabricate light-emitting and laser diodes, while alloys with $Zn_{0.5}Si_{0.5}N$ can provide ultraviolet light emission. A heterojunction transistor structure will rely on gallium nitride (GaN) or aluminum gallium nitride (AlGaN) as the second member of the junction pair. ternary nitrides are excellent candidate for serving as transistor bases or channels since they have smaller bandgaps than corresponding binaries while being very closely lattice matched, insuring high gain and high speed operation. $Zn_{0.5}Ge_{0.5}N$ can also serve as the charge storage reservoir for a cold cathode structure based on the negative electron affinity of AlN.

Our efforts have utilized plasma-enhanced metalorganic chemical vapor deposition, a technology we have been developing for the growth of stoichiometric binary nitrides. Deposition of $Zn_{0.5}Ge_{0.5}N$ films has required the substitution of Zn and Ge precursor sources in place of the organo-gallium flow, while maintaining a high flow rate of activated nitrogen species. Phase I investigations found conditions, basically the required substrate temperature and the II/IV ratio in the gas phase, which have yielded excellent quality single crystal $Zn_{0.5}Ge_{0.5}N$ films. These films have been characterized by several structural, optical, and electrical measurements which indicated film quality. In Phase II, reactor conditions for depositing $Zn_{0.5}Ge_{0.5}N$ films will be optimized and doping studies will commence, to establish preparation conditions for demonstrating high brightness blue light-emitting and laser diodes. We anticipate that n- and p-type doping in $Zn_{0.5}Ge_{0.5}N$ can be chosen by controlling the stoichiometry, rather than with extrinsic elements. Heterojunctions with lattice-matched GaN and nearly lattice-matched AlGaN films will be investigated. GaN and AlGaN will find service as cladding layers in graded index separate confinement heterostructure blue diode lasers.

Blue diode lasers based on $Zn_{0.5}Ge_{0.5}N$ will find critical Air Force use in providing secure satellite communications, including satellite links to subsurface seacraft. They will provide the blue light source for high brightness flat panel displays to be used in aircraft cockpits where readability of displays in direct sunlight is a critical consideration. Commercial applications of blue diode lasers for displays, optical memories (CD players), and indicator lights will be abundant.

HIGH TEMPERATURE HETEROJUNCTION TRANSISTORS WITH HIGH GAIN AND WIDE BANDWIDTH

1. SUMMARY OF RESULTS

We have successfully grown the world's first single crystal thin films of $Zn_{0.5}Ge_{0.5}N$. There is no evidence that any other investigators have ever produced single crystal films of this ternary nitride material before us. We have found that the growth temperature must be at least 650° C in our plasma-enhanced MOCVD system to deposit films of $Zn_{0.5}Ge_{0.5}N$ with excellent crystal quality. Strong x-ray diffraction spectra have been obtained under these conditions for films grown on (0001) sapphire substrates. Only a single orientation for the film material is indicated, with the c-axis perpendicular to the substrate surface. A reflection high energy electron diffraction study performed at Air Force Rome Laboratories has confirmed that our $Zn_{0.5}Ge_{0.5}N$ films are excellent single crystals. $Zn_{0.5}Ge_{0.5}N$ possesses the same wurtzite lattice as GaN, and has lattice parameters $a = 3.1826\text{\AA}$ and $c = 5.2132\text{\AA}$; the a parameter differs from GaN by only 0.2%. The bandgap of $Zn_{0.5}Ge_{0.5}N$ is 2.8 eV, giving band-to-band optical transitions at 442 nm in the deep blue region of the spectrum, which should lead to the production of a new class of bright blue light-emitting and laser diodes. The c/a ratio for $Zn_{0.5}Ge_{0.5}N$ is 1.638, indicating a rhombohedral expansion compared to GaN ($c/a = 1.626$), and therefore suggesting important nonlinear optical properties for this new material. $Zn_{0.5}Ge_{0.5}N$ films were also deposited on pre-grown GaN samples, and these films were also single crystal in nature. Thus the development of high performance modulation-doped-field-effect-transistors (MODFETs) and heterojunction-bipolar-transistors (HBTs) can be expected.

2. STATEMENT OF THE PROBLEM

2.1 High Performance Electronic Amplifier Devices

Although the III-V nitrides possess many desirable properties for application to high temperature electronic devices,¹ the achievable gain and bandwidths will remain limited unless heterojunction transistors can be manifested. Heterojunction transistors are discussed in some detail later in Section 8.1. In fact, AlGaN/GaN heterojunctions have already been reported, but aluminum nitride alloys generally suffer from low conductivity, and for alloys featuring 30% Al, the resistivity approaches $10^4 \Omega\text{-cm}$,² such highly resistive material will certainly give contact resistance problems which can compromise device bandwidths. Therefore, the objective of this program has been to develop deposition conditions for novel ternary nitride semiconductors consistent with the stringent requirements for both HBTs and MODFETs that can function at high speed with high gain in environments having elevated temperatures. Obviously, a necessary member material for these devices is gallium nitride (GaN), a semiconductor with a bandgap of 3.4 eV. We have worked to produce a lattice matched nitride with a smaller bandgap that can provide the potential barrier required for controlling the flow and velocity of charge carriers in these devices to function as the base of a high-temperature HBT, or as the channel in a MODFET.

The obvious nitride materials with bandgaps that are smaller than GaN that have already been investigated by several researchers^{3,4} are members of the alloy series $In_xGa_{1-x}N$, in analogy with GaAs/InAs alloys. Certainly, the $In_xGa_{1-x}N$ alloys provide a wide range of choices of bandgaps,

with GaAs/InAs alloys. Certainly, the $In_xGa_{1-x}N$ alloys provide a wide range of choices of bandgaps, ranging from 1.9 eV (InN) to 3.4 eV (GaN). Unfortunately, in analogy with the GaAs/InGaAs alloy series, InN has a significantly larger lattice parameter than GaN ($a=3.548\text{\AA}$ vs. $a=3.189\text{\AA}$, respectively), and therefore such alloys grown on GaN must suffer from increased numbers of structural (and hence electrically active) defects due to the mismatch. For our program we have asserted that it is more beneficial to pursue the growth of the stoichiometric compound $Zn_{0.5}Ge_{0.5}N$, which may be closely lattice matched to GaN. Consequently the major thrust of this Phase I program has been centered on defining deposition parameters for preparing epitaxial thin films of $Zn_{0.5}Ge_{0.5}N$ to form heterojunctions with GaN.

2.2. Blue Light-emitting and Laser Diodes

There are many military and commercial uses for blue light sources. Blue light-emitting diodes can function as simple indicator lights; or can be incorporated into complex flat panel displays. Blue diode lasers allow much greater storage densities for optical memories, while providing more secure satellite communications scenarios, including secure data links to submarines. In recent years, Japanese researchers have built upon Paul Maruska's seminal accomplishments from 1968 to 1974 in defining conditions for the growth and fabrication of blue GaN LEDs to recently produce high brightness commercial products. Present GaN/InGaN blue LEDs from Nichia Industries operating at 3.6 volts bias and drawing 20 mA emit a luminous intensity of 2 candelas with a conversion efficiency of 9%.⁵ They also have developed green GaN/InGaN LEDs, suitable for use as traffic lights, emitting a luminous intensity of 12 candelas with a conversion efficiency of 6%. The active InGaN layers are of course situated under compressive strain. Long term stability of these strained structures may be an issue, while optical scattering from mismatch-induced defects is bound to compromise laser performance.

NZ Applied Technologies has now developed the growth technology for preparing $Zn_{0.5}Ge_{0.5}N$, a blue material closely related to GaN, but one which offers additional degrees of freedom in choosing desirable optical and electrical properties. Because we have determined that $Zn_{0.5}Ge_{0.5}N$ is almost exactly lattice-matched with GaN ($\Delta a = 0.2\%$), there is essentially no strain in heterostructures. Because the band edge of $Zn_{0.5}Ge_{0.5}N$ is located at 440 nm in the blue, there is no requirement for adding recombination (color) centers to downshift the emission from the ultraviolet, as in $In_{0.20}Ga_{0.80}N$.

3. BACKGROUND

3.1. Emerging Devices

3.1.1 Light Emitting Devices

In 1994 Nakamura⁶ announced his demonstration of the world's first truly high brightness blue light-emitting diode (LED) with luminous intensity exceeding 1 candela, and external quantum efficiency greater than 2%, based on gallium nitride. Early in 1996, Nakamura announced the first gallium nitride based room temperature injection laser.⁷ Nakamura's device are prepared using alloys of aluminum nitride (AlN), gallium nitride (GaN), and indium nitride (InN). Until the advent of nitride LEDs, all commercial LEDs as well as diode lasers have been based on III-V materials involving phosphorus or arsenic (basically

various alloys of aluminum arsenide, gallium arsenide, indium arsenide, aluminum phosphide, gallium phosphide, indium phosphide). These traditional materials give very bright light emission in the near infrared (1550 to 750 nm) as well as visible red, orange and yellow light emission. However, although green light is available from GaP LEDs, these GaP devices are always low intensity (<0.1 candela) and not even truly green (only yellow-green). GaP lasers have not been demonstrated, and are unlikely due to the indirect bandgap. Although blue diode lasers have been demonstrated with ZnSe, they are extremely short-lived (usually only a few seconds), and only operate cw at reduced temperatures.⁸ In light of these deficiencies, it is clear that the wide bandgap nitrides constitute a unique new materials series with remarkable properties.

Red LEDs have been available for many years in high brightness forms. However, in order to assemble flat display panels using LEDs, bright blue and green sources are required, which heretofore have been lacking. Furthermore bright blue and green light sources are needed for indicator lights, including traffic lights and automobile dashboard lights. Consequently, the Japanese announcements of bright blue and green nitride LEDs and LDs have sparked tremendous interest in the family of III-V nitride semiconductors.

3.1.2 Electronic Amplifiers and Switches

Because the nitride semiconductors have wider bandgaps than silicon or the III-V arsenides and phosphides, electronic amplifier and switching devices based on nitrides can remain operational at much higher temperatures. Furthermore, these materials have higher thermal conductivities than Si, GaAs, or InP, and therefore can handle greater power levels. Simple GaN field-effect transistors using Schottky barrier gate contacts have been reported.⁹ Much superior operating characteristics are generally expected from transistors featuring heterojunctions between a wider bandgap charge supply layer and a narrower bandgap undoped charge transit channel, a so-called "high electron mobility transistor" or HEMT (also called a MODFET). Such a HEMT using a GaN channel and an AlN-GaN alloy film as the charge supply film has now been demonstrated.¹⁰

3.1.3 Data Storage and Spectroscopy

Since the focussed spot size of a light beam is inversely proportional to the square of the wavelength, blue or ultraviolet laser diodes would allow a great increase in the storage density of optical memories (including compact disks) - a shift from the 900nm of traditional GaAs diode lasers to a 300 nm emission wavelength from a nitride diode laser would give a factor of 10 increase in storage density. Furthermore, wide bandgap materials such as the nitrides of aluminum, gallium, and indium have non-centrosymmetric crystal structures, making them candidates for use as nonlinear optical materials for up-shifting or down-shifting the emission wavelengths of other types of lasers.

3.1.4 Other Applications

Other applications for III-V nitrides can be listed. Because most of the alloys in this materials family are transparent to at least part of the visible spectrum, they can be used for fabricating waveguides and Bragg mirrors. Such mirrors can be used as optical filters to divide

white light in red, green, and blue segments. Additionally, these materials can be used as detectors which are not affected by visible radiation, such as sunlight.¹¹

Finally, the wide bandgap member AlN, ($E_G = 6.2$ eV), appears to exhibit negative electron affinity, which implies that the conduction band in AlN is above vacuum level, so that any electrons which are introduced into AlN will be ejected into vacuum without restraint. Thus the nitride materials may find use as cold cathode field emitters for flat panel displays and high performance microwave vacuum tubes.

3.2. Materials Preparation

3.2.1 Gallium Nitride

The preparation of GaN was first reported in 1932 by Johnson, Parsons, and Crew¹² who reacted gallium metal with ammonia to produce GaN powder. Determination of the wurtzite crystal structures of both GaN and InN using powder samples was first reported in 1938.¹³ Although several more papers were published on powder nitride samples in the next thirty years, it was not until 1969 that Maruska at RCA Laboratories first developed a method for the growth of single crystal epitaxial films of GaN.¹⁴ Maruska reacted gallium chloride vapors with flowing ammonia in an open tube furnace, and deposited films on single crystal sapphire substrates. Maruska first reported the fabrication of blue and violet GaN LEDs in 1973,¹⁵ and created the model for their operation based on tunneling through a potential barrier.¹⁶ Subsequently, the use of metalorganic chemical vapor deposition of gallium and aluminum nitride was developed,¹⁷ and has become the preparation method of choice today. Presently, materials preparation of GaN and $Al_xGa_{1-x}N$ is undergoing rapid development.¹⁸

3.2.2. Listing of Problem Areas for III-V Nitrides

Despite great progress in improving the methods of crystal growth for the nitride semiconductors and hence the development of both laboratory and commercial devices, there are many serious problems that remain with these materials. Controlling the electrical conductivity has always been an issue. Maruska found that his GaN films were always highly conducting, with only n-type (electron) conduction possible. He found that the usual p-type dopant for III-V compounds, zinc, only makes GaN highly resistive, with no appreciable hole currents. Subsequently, he introduced magnesium as a potential p-type dopant, and prepared blue LEDs visible in a lighted room based on a field-effect in insulating Mg-doped GaN.¹⁹ Much later, Nakamura found that by performing a one-hour anneal of Mg-doped GaN films at 700° C, he could render them p-type conducting.²⁰ However, only a small fraction of the Mg ions contribute to the hole conductivity, while the remainder form deep levels responsible for the light emission at blue/violet rather than ultraviolet wavelengths. Thus the light emission from GaN-based LEDs is very broad, and band-to-band recombination at the band edge at 365 nm in the ultraviolet is very weak. It has not been possible to bring n-type conductivities below the level of $1 \times 10^{17} \text{ cm}^{-3}$, primarily due to nitrogen vacancies; thus enhancement mode transistors and p-i-n diode detectors have not been possible. All longer wavelength work has involved alloying InN with GaN, but InN has a much larger lattice constant than GaN ($a=3.548\text{\AA}$ vs. $a=3.189\text{\AA}$, respectively) which means that $In_xGa_{1-x}N$ films grown between GaN layers are under large compressive stresses. Furthermore, the equilibrium vapor pressure of nitrogen over InN

is extremely high, and InN rapidly dissociates when held at temperatures above 500°C. Most discussions of the growth of InN refer to inclusions of metallic indium in the films, along with great concentrations of nitrogen vacancies in the accompanying InN material. Thus work based on MOCVD of $In_xGa_{1-x}N$ alloys typically must keep the In content below 20%, and usually does not exceed about 12%, to control the nitrogen vacancy problem. Thus alloy bandgaps must typically remain above 3.0 eV, and even so, low growth temperatures are necessary, where the decomposition of ammonia is inefficient, and where poor surface mobility of reacting species leads to poor quality or polycrystalline films.

Finally, there is no particular lattice matching between GaN films and sapphire substrates. Thus much effort is presently being given to preparing new materials for substrates and in discovering alternative growth procedures which can decrease the densities of misfit dislocations in GaN films.

3.2.3. Approach to Improved Devices

In light of these problems, other related semiconducting nitrides become of interest. It is important to consider that the III-V compounds themselves are extensions of the simple diamond-like semiconductors Si, Ge, and α -Sn. Due to the rules of chemical bonding, these materials follow the four-electrons-per-site rule, and this accounts for their semiconducting and doping properties, including the changes in bandgap. Every anion is tetrahedrally bonded to four cations, and every cation is tetrahedrally bonded to four anions. When a member of Group III plus a member of Group V is substituted for a pair of the Group IV elements, the tetrahedral bonding arrangement is maintained, but many new properties become available. Examples include AlP for Si, and GaAs for Ge. These new semiconductors include larger and often direct bandgaps, and higher carrier mobilities. Even more possibilities become available if we substitute a pair consisting of a Group II plus a Group IV element for the Group III member (substitutions of the Group V are not possible). Two examples of ternary semiconductors which have been prepared include $(Zn_{0.5}Si_{0.5})P$ and $(Zn_{0.5}Ge_{0.5})As$, where for example $(Zn_{0.5}Ge_{0.5})As$ is the ternary analog of GaAs. This same type of II-IV for III substitution can be made for the nitride semiconductors, e.g., $Zn_{0.5}Ge_{0.5}N$ for GaN, or $Zn_{0.5}Si_{0.5}N$ for AlN.

3.2.4 $Zn_{0.5}Ge_{0.5}N$

There are relatively few reports on the preparation or properties of $Zn_{0.5}Ge_{0.5}N$. Maruska prepared $Zn_{0.5}Ge_{0.5}N$ in thin film form by reacting elemental zinc and germanium (transported as their chlorides) with ammonia gas in a tube furnace.²¹ He used sapphire as a substrate, and produced polycrystalline thin films with a pale yellow color. He placed the bandgap at 2.67 eV, based on optical transmission measurements. Because he had rather poor control over the activity of the reactants, his material was far from ideal.

Maunaye et Lang²² prepared $Zn_{0.5}Ge_{0.5}N$ by reacting zinc metal with Ge_3N_4 at 750°C. Their product was contaminated with excess Ge. Very recently, Endo et al²³ mixed Zn_3N_2 with either Si_3N_4 or Ge_3N_4 powders and heated them at 1000-1600°C under an extremely high pressure of 4-6.5 GPa for several hours. They report recovering both $Zn_{0.5}Ge_{0.5}N$ and $ZnSiN_2$. For $ZnSiN_2$, they determined the lattice parameter $a = 3.035\text{\AA}$, indicating that alloys would have a smaller lattice parameter, as expected. Endo's samples of $Zn_{0.5}Ge_{0.5}N$ were black and

conducting, probably due to a lack of stoichiometry (nitrogen loss during the reaction). Grekov et al have presented a detailed discussion of the structure and chemical bonding in ternary nitrides.²⁴ $Zn_{0.5}Ge_{0.5}N$ has the sodium β -ferrite rhombohedral structure, the hexagonal equivalent of cubic chalcopyrite. The cations, Zn and Ge, are ordered in the $Zn_{0.5}Ge_{0.5}N$ structure.²⁵ The crystal structure is shown in Figure 1. Ordering of the cations is accompanied by deviations from the ideal atomic positions of wurtzite. $Zn_{0.5}Ge_{0.5}N$ exhibits significant rhombic expansion, and therefore may be a potentially useful material for non-linear optical effects.

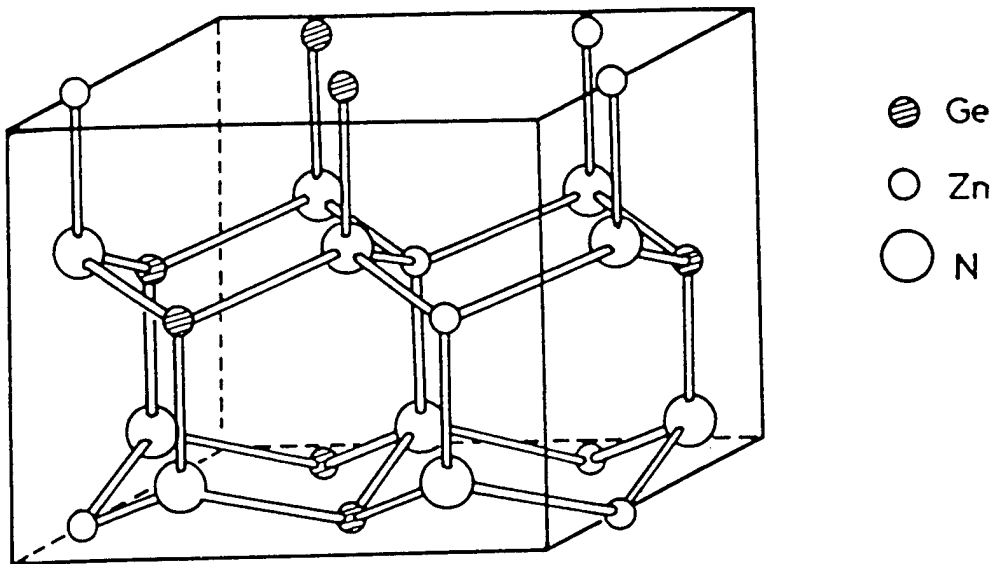


Figure 1. The crystal structure of $Zn_{0.5}Ge_{0.5}N$.

3.2.5 $Zn_{0.5}Ge_{0.5}P$

A brief discussion of $Zn_{0.5}Ge_{0.5}P$ is in order at this point. This material is used extensively for frequency shifting applications due to its high birefringence and substantial nonlinear optical figure of merit.²⁶ Bulk crystals are usually grown from the melt. Bliss *et al* at Air Force Rome Laboratories have recently announced a chemical vapor transport process based on iodine for growing $Zn_{0.5}Ge_{0.5}P$.²⁷ MOCVD growth of $Zn_{0.5}Ge_{0.5}P$ has been reported by Bachmann's group at North Carolina State University.²⁸ All MOCVD samples proved to be low resistivity p-type, with carrier concentrations around $1 \times 10^{18} \text{ cm}^{-3}$; in contrast, samples prepared by sublimation and transport in a closed tube proved to be n-type. Therefore, changes in the growth conditions can shift the conductivity type for $Zn_{0.5}Ge_{0.5}P$ from p- to n-type; clearly, the Zn/Ge ratio will be critical. A deficiency of Zn leads to vacancies on the cation lattice and hence the formation of acceptors (p-type). A stoichiometric Zn/Ge ratio with P vacancies will give donors (n-type). *The extra degree of freedom presented by the ternary II-IV-V compound can allow n- and p-type conductivity to be manifested without the need for extrinsic dopants.* Thus by analogy, $Zn_{0.5}Ge_{0.5}N$ may also provide both types of doping with control afforded

through manipulation of the Zn/Ge ratio in the vapor.

4 TECHNICAL APPROACH

NZ Applied Technologies has been in a unique position to develop $Zn_{0.5}Ge_{0.5}N$ deposition technology. Our original PE-MOCVD reactor has been designed specifically for the growth of III-V nitrides, and the availability of a source of activated nitrogen (rather than ammonia) typically has allowed growth to be performed at relatively low temperatures. Controllable parameters affecting the quality of crystal growth in NZ Applied Technologies's reactor have included the substrate orientation, the substrate temperature, the ratios of source gas constituents, the total gas pressure, and the microwave power for generating the nitrogen plasma. These parameters have been scrutinized in the course of the program to insure the deposition of high quality films.

We have routinely used a remote microwave source to activate nitrogen, and the kinetic energy imparted to the nitrogen species reduces the requirements for thermal energy that would be necessary to allow nitrogen atoms to migrate on the growing surface. The excess energy allows growth to be performed at lower substrate temperatures, which in turn reduces the rate of re-evaporation of nitrogen, since the vapor pressure drops with temperature. These growth conditions have allowed us to prepare GaN films with n-type carrier concentrations as low as $1 \times 10^{17} \text{ cm}^{-3}$.²⁹

$Zn_{0.5}Ge_{0.5}N$ has never before been prepared by MOCVD. Thus we have had to start with basic choices for the growth process, including choices of precursors, choices of flowrates, choices of cleaning procedures, choices of growth temperatures, choices of substrates. Our basic approach involves the selection of appropriate Zn and Ge precursors. Two metalorganic zinc sources are commercially available, dimethylzinc (DMZ) and diethylzinc (DEZ). DEZ is appropriate for our system because at a bubbler temperature of 10° C, it has a vapor pressure of 6.8 mm of Hg. DMZ is much more volatile, already having a vapor pressure of 57.4 mm of Hg at -15° C. DMZ would be expected to coat the entire growth chamber with metallic zinc during the course of growth runs.

For germanium, there are both metalorganic and hydride choices. The commercial MO source, tetramethylgermanium, already has a vapor pressure of 10 mm of Hg at -45° C. Thus it would be very difficult to handle. GeH_4 is a highly toxic gas in pure form, but can be readily handled when diluted to a level of 0.1% in helium. Thus we have chosen to use germane.

Basically, sapphire substrates have been used. Sapphire, of course, is the usual substrate employed for the growth of nitrides. For growth temperature, we have learned that both Zn_3N_2 and Ge_3N_2 are volatile above 600° C, while Ge_3N_4 decomposes at 450° C. Therefore, we estimate that a relatively low growth temperature for $Zn_{0.5}Ge_{0.5}N$ will be preferred. Also, since Zn is far more volatile than Ge, we expect that more Zn than Ge will be needed in the reaction zone. For reference, it is known that the Zn/Ge ratio is a critical parameter in the growth of single crystal films of $ZnGeP_2$, a related semiconductor.³⁰

All substrates have been thoroughly cleaned and degreased by traditional methods using solvents and acids. Substrates were then placed in the reaction chamber and heated for a pre-

treated at various temperatures and times. The heater was then set at the growth temperature, and the Zn and Ge precursor flows were initiated. At the conclusion of a run, the samples were removed from the reaction chamber and subjected to characterization procedures.

5 PHASE I TECHNICAL OBJECTIVES

The specific technical objectives that have been pursued in Phase I were:

1. To design conditions for successful deposition of $Zn_{0.5}Ge_{0.5}N$ epitaxial films by PE-MOCVD;
2. To acquire sapphire wafers with the required orientation, and prepare the surface by plasma nitriding;
3. To deposit GaN buffer layers, and assess their properties;
4. To grow GaN layers with excellent crystal structures at relative low temperatures ($\sim 850^{\circ}C$);
5. When high quality GaN films have been achieved, to deposit epitaxial $Zn_{0.5}Ge_{0.5}N$ films, 1 - 2 μm thick;
6. To evaluate the structural, electrical, and optical properties of the $Zn_{0.5}Ge_{0.5}N$ films.

These tasks are designed to answer the following questions:

- Can $Zn_{0.5}Ge_{0.5}N$ films of high crystalline perfection be deposited on buffered sapphire substrates?
- How do the properties of these films compare with those produced by other growth techniques?
- What magnitudes of electron mobilities are possible in $Zn_{0.5}Ge_{0.5}N$?
- Can crystalline imperfections be controlled to the extent required in a minority carrier device?

6 TECHNICAL RESULTS

6.1 Overview of Film Growth

The original version of NZ Applied Technologies' PE-MOCVD reactor which was used for growing all the samples for this study did not have sufficient ports for allowing the connection of a gallium precursor and a zinc precursor simultaneously. Therefore, a number of films of GaN had to be grown before the work on $Zn_{0.5}Ge_{0.5}N$ began. The GaN films were stored in a clean drybox for later use. WE HAVE NOW REBUILT THE ENTIRE REACTOR. THE DEPOSITION CHAMBER HAS BEEN COMPLETELY REDESIGNED AND INSTALLED. IT IS NOW CAPABLE OF HANDLING 2 AND 3" DIAMETER WAFERS. ALL OF THE PLUMBING HAS BEEN REWORKED, AND THERE NOW ARE PORTS AVAILABLE FOR 4 METALORGANIC SOURCES SIMULTANEOUSLY, AS WELL AS 4 GASEOUS SOURCES. THUS NZ Applied Technologies IS READY TO PROCEED FULL SCALE WITH A PHASE II PROGRAM.

A schematic diagram of our reactor configuration is shown in Figure 2.

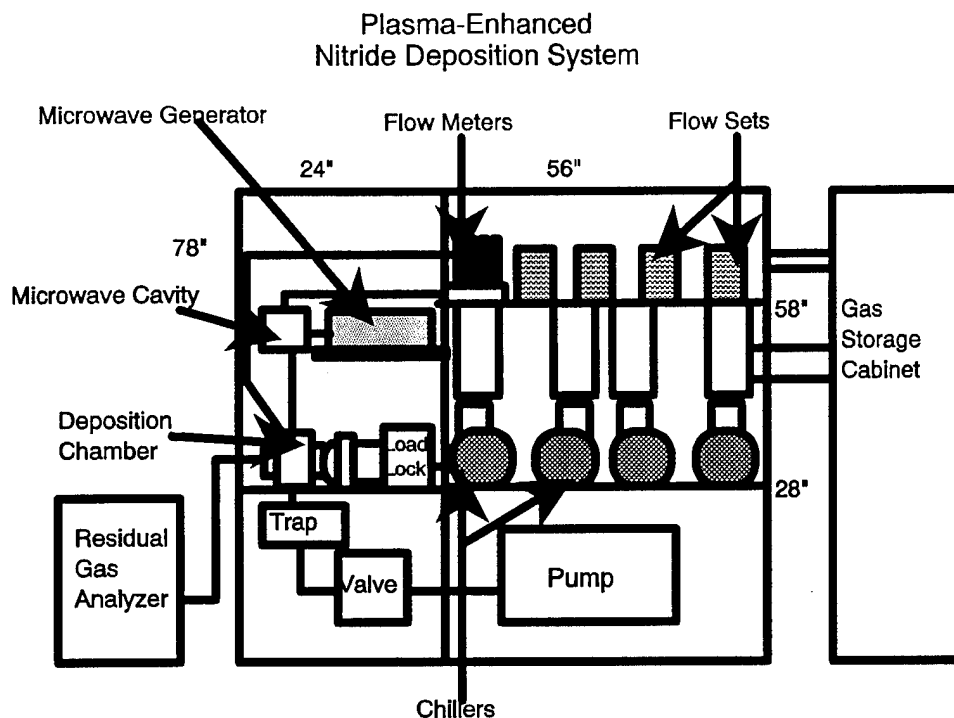


Figure 2. NZ Applied Technologies expanded MOCVD reactor for nitride growth.

The Zn and the Ge sources were then added to the PE-MOCVD reactor. All of the stainless steel tubing and valving associated with these flow lines were thoroughly cleaned and leak-tested. In initial runs, the plasma gas was a mixture of 15% hydrogen in nitrogen. We have found that for growth of GaN in our system, the presence of hydrogen atoms is vital for effective removal of residual organics in the form of CH_4 . Table I presents important parameters for all of the significant runs. Basically, all early runs resulted in the deposition of Ge_3N_4 because of the presence of a hydrogen plasma which scavenged most of the zinc. When a source of pure nitrogen was substituted for the H_2/N_2 mixture, films of $\text{Zn}_{0.5}\text{Ge}_{0.5}\text{N}$ were grown. Although some of the deposits proved to be polycrystalline; significantly, runs ZNG114 and ZNG116 yielded what we believe to be the *world's first single crystal films of $\text{Zn}_{0.5}\text{Ge}_{0.5}\text{N}$* .

6.2 Initial Results: First Single Crystal Films of $\text{Zn}_{0.5}\text{Ge}_{0.5}\text{N}$

These preliminary results are very exciting. We have found conditions for growing single crystal films of $\text{Zn}_{0.5}\text{Ge}_{0.5}\text{N}$, and have demonstrated two different orientations for the c-axis, perpendicular and parallel to the substrate surface. When the single diffraction peak occurs at 34.4° , then the orientation is (002). When the single peak is at 57.95° , then the orientation is (110). Notice that the (110) hexagonal orientation indicates that the a-axis is perpendicular to the substrate surface. This finding may be very significant for non-linear optical effects in $\text{Zn}_{0.5}\text{Ge}_{0.5}\text{N}$, because with this orientation, the polarization of the E-vector for an incoming laser source can be made either ordinary (facing an in-plane a-direction) or extra-ordinary (facing the

in-plane c-axis). This is very important for phase matching in second harmonic generation. The x-ray diffraction pattern of $Zn_{0.5}Ge_{0.5}N$ film ZNG114 is shown in Figure 3. The two strong peaks are due to the sapphire substrate. Figure 4 shows the diffraction pattern of ZGN116, where again the sapphire peaks are apparent, but where now the $Zn_{0.5}Ge_{0.5}N$ peak is at 58° , indicating a (110) orientation for the film.

TABLE I
 $ZnGeN_2$ Film Growth

Run Numb.	Substrate	Pre-treat °C, min.	Growth temp., °C	Plasma N_2 flow, sccm	DEZ, °C bubbler, sccm	GeV_4 , 0.1% / He sccm	Run time, hr.	EDX, At% Zn, Ge	Resist ance	Color	Crystal Struct., 2θ
101	Sap., Si	670, 60	400	300*	-15, 50	16	3½	2.4, 97.6			-
102	Sap., Si	670, 150	600	300*	10, 50	8	4½	none			-
103	Sap., Si	600, 60	400	300*	10, 100	16	3½	mostly Ge			-
114		650, 50	550	250	10, 100	16	2	52.9, 47.1		yellow	Single, 34.6 (002)
115	Sap., Si	660, 45	550	300	10, 100	20	5	48.3, 51.7	∞	yellow	Poly
116	Sap., GaN620	660, 30	550	300	10, 100	18	5	48.2, 51.8			Poly GaN; Sap, single 58.1 (120)
271	Sap., GaN735	660, 30 550, 10	550	300	10, 100	16.8	5	49.9, 50.1			GaN: not resolve. Sap, single 58.1 (120)
282	Sap., GaN735	660, 40 550, 30	550	300	10, 100	16.8	8½	51.0, 49.0		yellow	GaN: not resolve. Sap, single 34.6 (002)
293	Sap., Si	660, 60	650	300	10, 100	16.8	5	40.5, 59.5		yellow	Sap, single 34.72 (002)
310				New N_2 cyl.				No film			
311				New N_2 Cyl.				No film			
312				New N_2 cyl				No film			
413	Sap., Si	660	500	300 (2nd N_2 cyl.)	10, 100	16.8	3½	48.9, 51.1 52.9, 49.6 (edge)		yellow	
414		660	610	300	10, 100	33.6	5½				
415		660	625	200	10, 50	16.8	5				Sap, single 34.6 (002)

Note: * = 15% H_2 in N_2 .

From the results on the diffraction pattern of polycrystalline $Zn_{0.5}Ge_{0.5}N$ film 115, we have been able to calculate the hexagonal lattice parameters. The diffraction pattern is shown in Figure 5. The radiation was from copper at 1.54059\AA . The observed peaks are given in Table 2. Peaks 3, 5, and 6 are due to the sapphire substrate. We noted a small angular discrepancy between our results for sapphire and the accepted literature values. Our diffraction results for a sapphire substrate without overgrowth is given in Table 3. The accepted values for sapphire are as follows. The (0006) diffraction peak is at $2\theta = 41.73^\circ$. The (00012) is at

90.79° for CuK α , and 90.99° for CuK β . Therefore, all of the Zn_{0.5}Ge_{0.5}N data was corrected according to the sapphire data.

Table 2.
X-ray Diffraction Study of Polycrystalline Zn_{0.5}Ge_{0.5}N

Peak Number	2θ	d, Å	Background I	Signal Peak	FWHM
1	34.651	2.5866	6	34	0.238
2	37.260	2.4113	5	42	0.086
3	42.162	2.1416	4	27929	0.167
4	58.153	1.5850	3	27	0.067
5	91.072	1.0793	14	13133	0.180
6	91.422	1.0761	14	1706	0.267

Table 3
X-ray Diffraction Study of Sapphire Substrate

Peak Number	2θ	d, Å	Background I	Signal Peak	FWHM
1	41.999	2.1495	5	5308	0.170
2	90.941	1.0805	18	1752	0.216
3	90.971	1.0803	8	1879	0.217
4	91.334	1.0769	7	460	0.385

Table 4 presents the indexed diffraction peaks for Zn_{0.5}Ge_{0.5}N from our study:

Table 4
Indexing of Zn_{0.5}Ge_{0.5}N Data

Peak number	2θ	d, Å, exper.	(hkl)	d, Å, calc.	Δ2θ
1	34.40	2.60696	(002)	2.60673	-.003
2	36.90	2.43588	(101)	2.43664	+.012
3	57.95	1.59136	(110)	1.59129	-.003

We find that a = b = 3.1826 Å and c = 5.2132 Å, and c/a = 1.638. These may be compared with the generally accepted unit cell parameters for GaN films, *viz.*, a = 3.189 Å and c = 5.185 Å, c/a = 1.626. The a-parameter mismatch is only 0.2%. There is a rhombohedral expansion in the lattice of Zn_{0.5}Ge_{0.5}N compared to GaN.

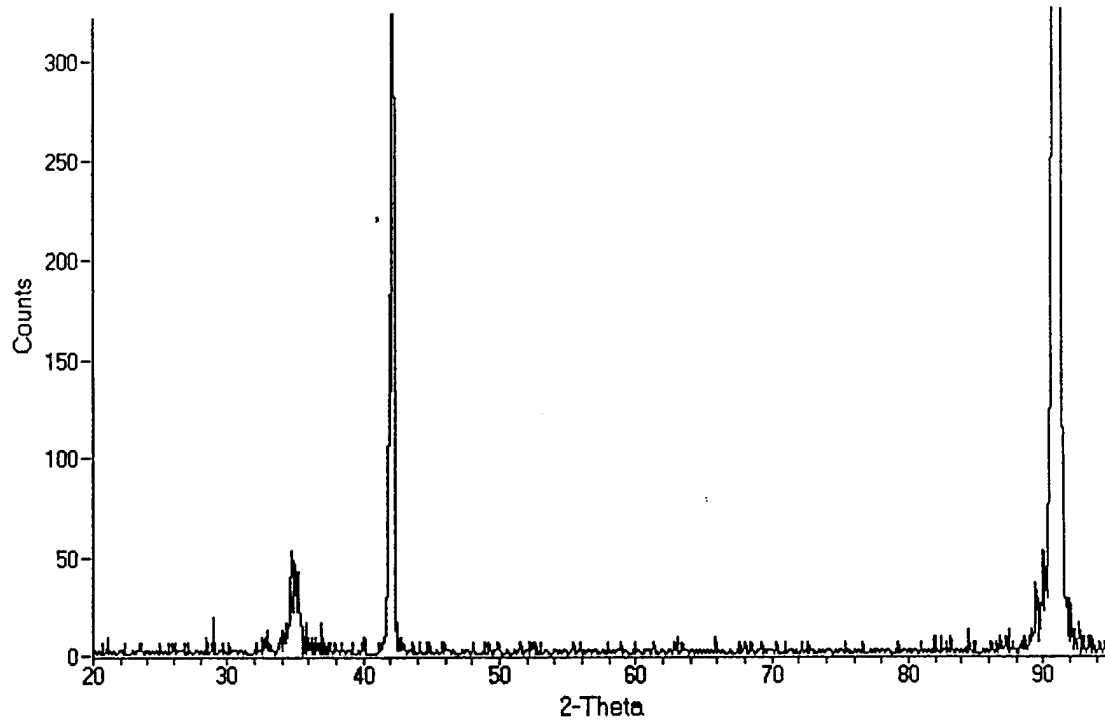


Figure 3. X-ray diffraction pattern of single crystal $Zn_{0.5}Ge_{0.5}N$ film with (002) orientation.

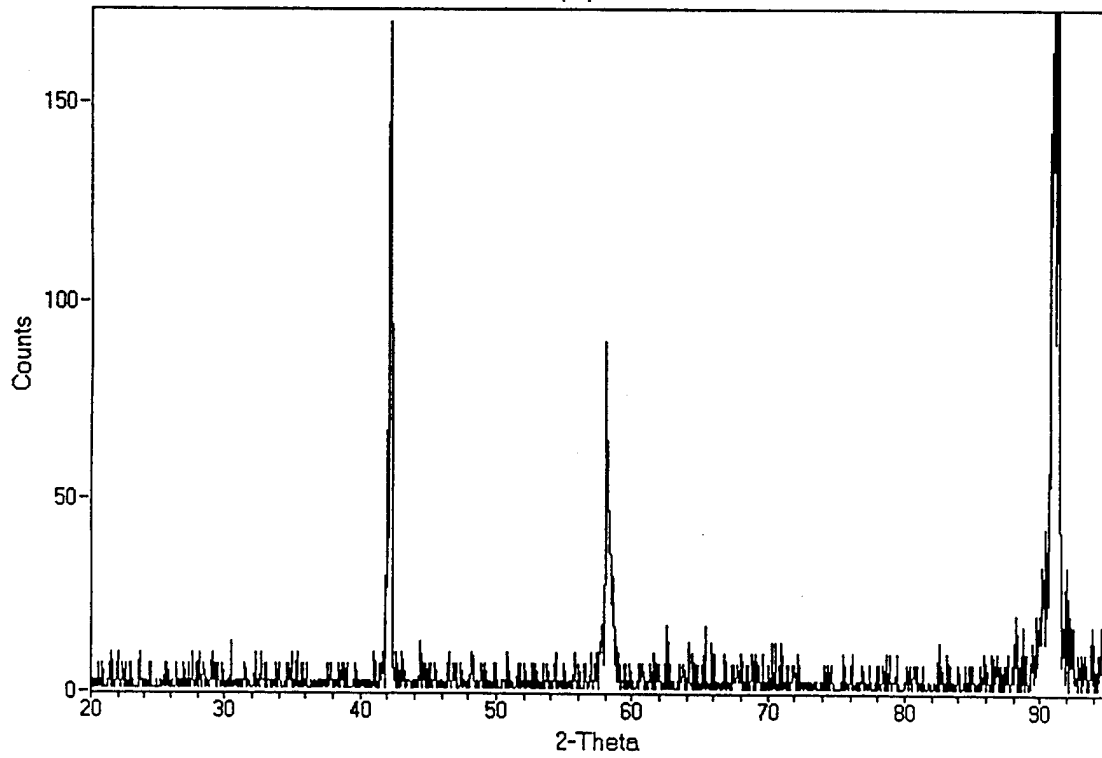


Figure 4. X-ray diffraction pattern of single crystal $Zn_{0.5}Ge_{0.5}N$ film with (110) orientation.

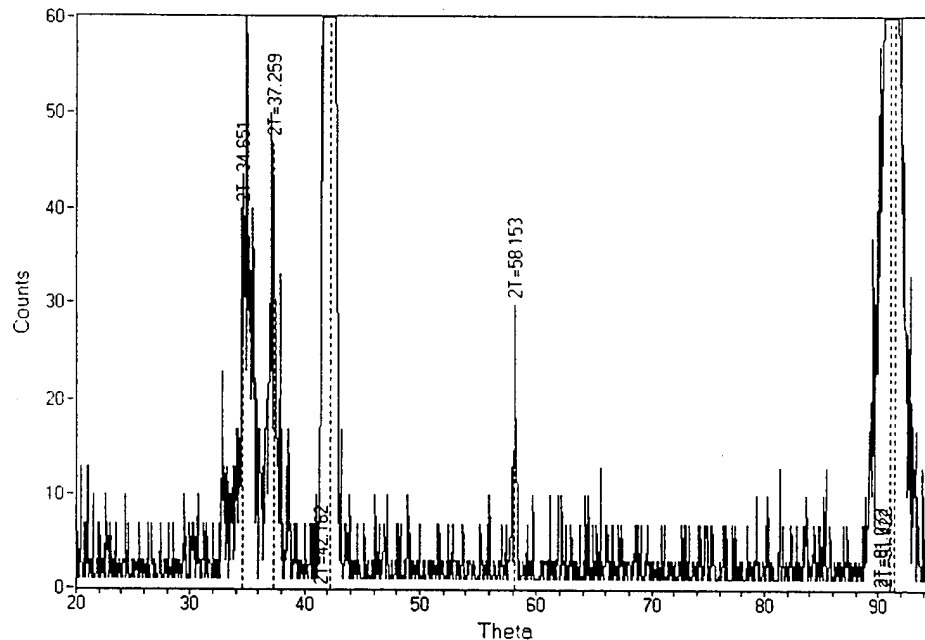


Figure 5. X-ray diffraction pattern of polycrystalline $\text{Zn}_{0.5}\text{Ge}_{0.5}\text{N}$ film

6.3 Improved Film Quality

We have found that raising the temperature of the substrate is critical for improving the quality of the films. For example, in our initial work, we performed the deposition of $\text{Zn}_{0.5}\text{Ge}_{0.5}\text{N}$ films at 550° C , using diethylzinc and germane, along with activated nitrogen from a plasma. Although x-ray $\Theta/2\Theta$ patterns were obtained for some of the films which indicated a single crystal orientation, the diffraction peaks were not very strong. We consider that although there was definitely a single-crystalline component in the films, there was also a possible amorphous matrix. In contrast, for films grown at 650° C , much stronger diffraction patterns have been obtained. Figure 6 shows the $\Theta/2\Theta$ plot for film 291, which was grown at 650°C on basal plane sapphire. The intensity is 3000 counts. For comparison, film 114 only showed 50 counts under the same conditions of test. The pattern is shown with greater resolution in Figure 7. Here we have indexed the $\text{Zn}_{0.5}\text{Ge}_{0.5}\text{N}$ (0002) peak at 34.726° , and the $\text{Zn}_{0.5}\text{Ge}_{0.5}\text{N}$ (0004) peak at 72.961° . The sapphire (00012) peak is visible at 90.8° . Figure 8 shows the $\text{Zn}_{0.5}\text{Ge}_{0.5}\text{N}$ (0002) peak in greater detail. Only a single peak can be discerned, indicating the excellent crystallinity of this deposit. ***There is no doubt that NZ Applied Technologies has now succeeded in preparing the world's first single crystal films of zinc germanium nitride.***

6.4 Growth of $\text{Zn}_{0.5}\text{Ge}_{0.5}\text{N}$ on GaN

We have also deposited $\text{Zn}_{0.5}\text{Ge}_{0.5}\text{N}$ films on gallium nitride. The GaN films were grown earlier as explained above, because the early version of our reactor did not have sufficient ports to include a gallium source. The x-ray diffraction pattern of the GaN deposit, which was grown on a sapphire substrate, is shown in Figure 9. The single crystal nature of the film is apparent. After the deposition of $\text{Zn}_{0.5}\text{Ge}_{0.5}\text{N}$ on this substrate, it was not possible to distinguish the two compounds, because the a-parameters differ by only 0.2% (3.189\AA and 3.1826\AA). This diffraction spectrum is shown in Figure 10.

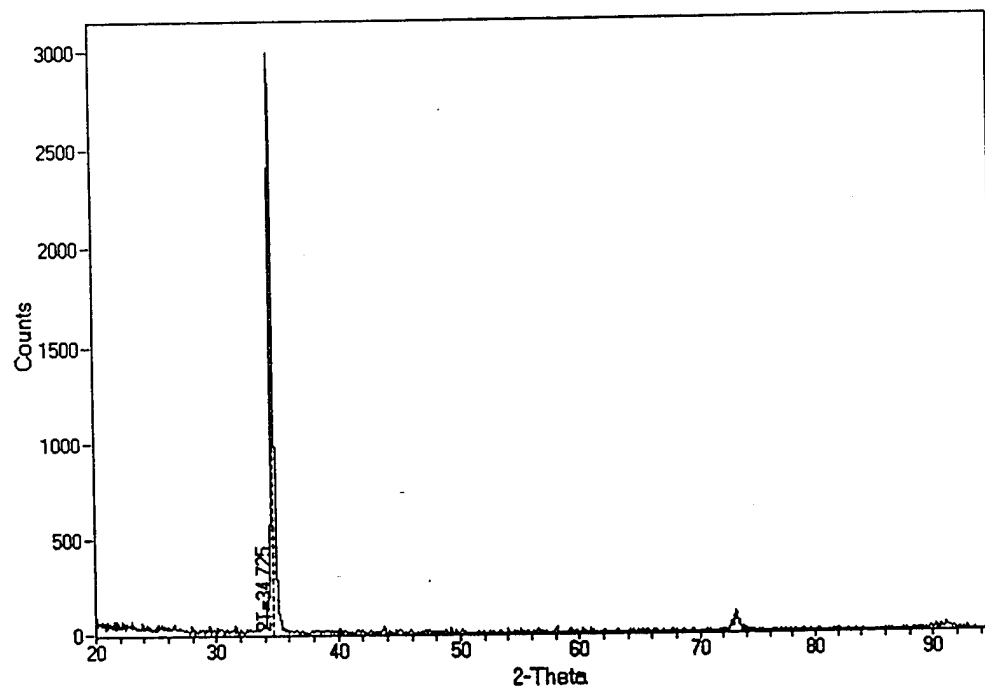


Figure 6. X-ray diffraction pattern of single crystal $\text{Zn}_{0.5}\text{Ge}_{0.5}\text{N}$ film 291 with (0002) orientation, grown at 650°C .

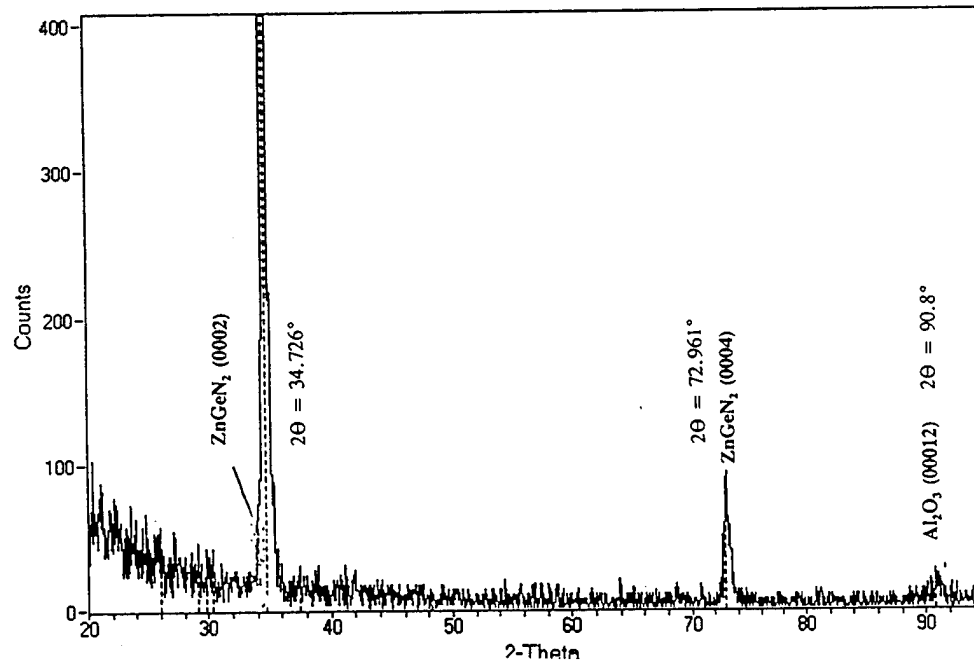


Figure 7. Increased intensity resolution for X-ray diffraction pattern of Figure 6, showing (0002) and (0004) peaks.

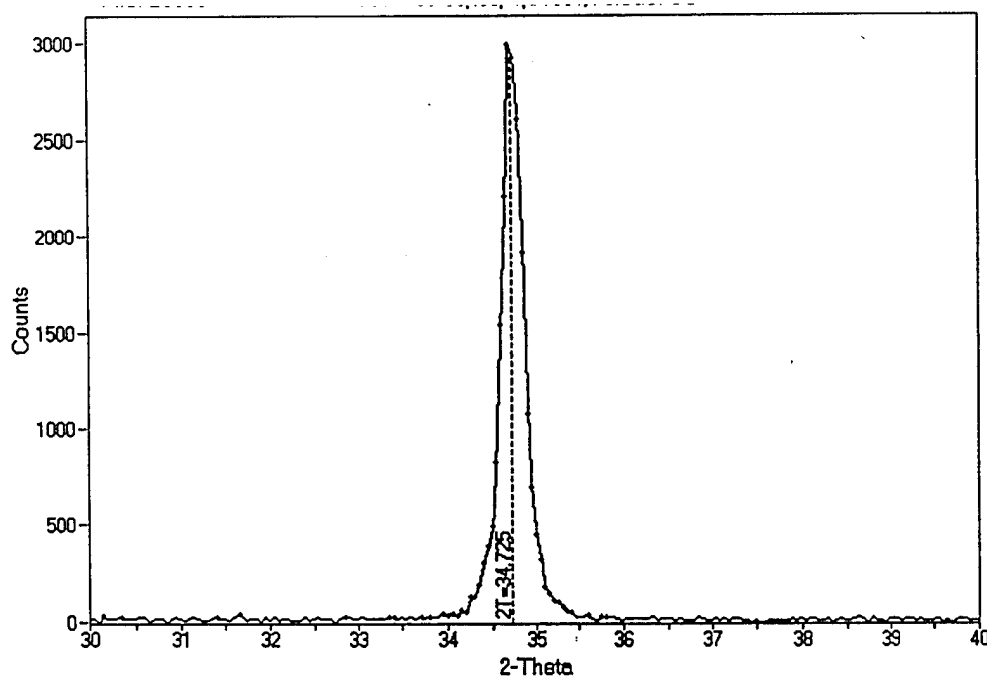


Figure 8. Increased angular resolution for X-ray diffraction pattern of Figure 6, indication a single peak at 34.725°.

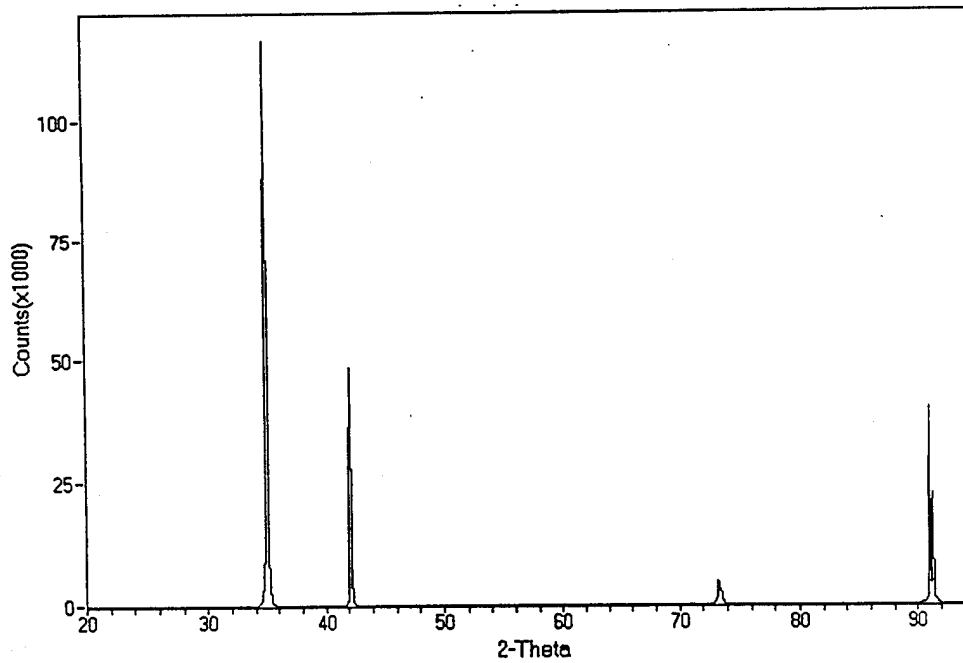


Figure 9. X-ray diffraction pattern for GaN film grown on (0001) sapphire

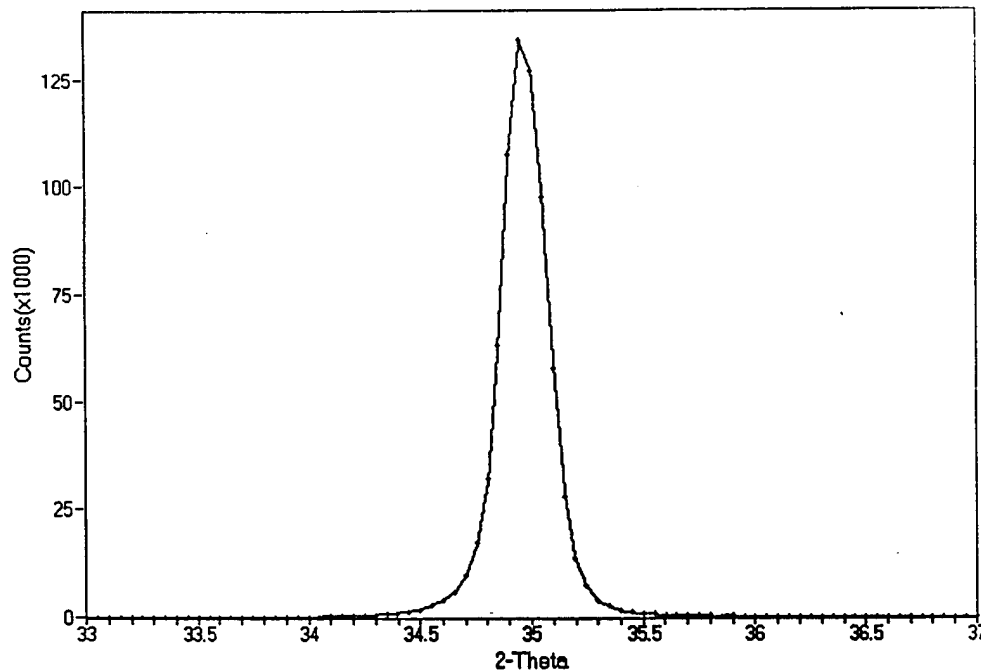


Figure 10. X-ray diffraction pattern for $Zn_{0.5}Ge_{0.5}N$ film grown on the GaN film analyzed in Figure 9. The $Zn_{0.5}Ge_{0.5}N$ and GaN peaks are indistinguishable.

The films were also studied in a JEOL Model 100-CX at Hanscom Air Force Base, under the guidance of Brian Demczyuk and John Larkin. The beam impingement angle was 1° , and the beam energies that were used included 20 and 100 keV. It is clear that a 20 keV beam will not penetrate through a $Zn_{0.5}Ge_{0.5}N$ to a film of GaN beneath it.

The reflection high energy electron diffraction (RHEED) pattern for sample 291 is shown in Figure 11. The beam energy was 100 keV. The bright spot pattern is due to $Zn_{0.5}Ge_{0.5}N$, while the dim fine points come from the sapphire substrate. The beam angle is basically orthogonal to the c-axis of the films, leading to a (10i0) RHEED pattern, which is rectangular. This pattern of spots assures that the $Zn_{0.5}Ge_{0.5}N$ is an excellent single crystal.

A RHEED pattern for one of the $Zn_{0.5}Ge_{0.5}N$ films grown on a GaN substrate is shown in Figure 12. Here, the beam energy was reduced to 20 keV to prevent penetration into the GaN. This film is also a good single crystal.

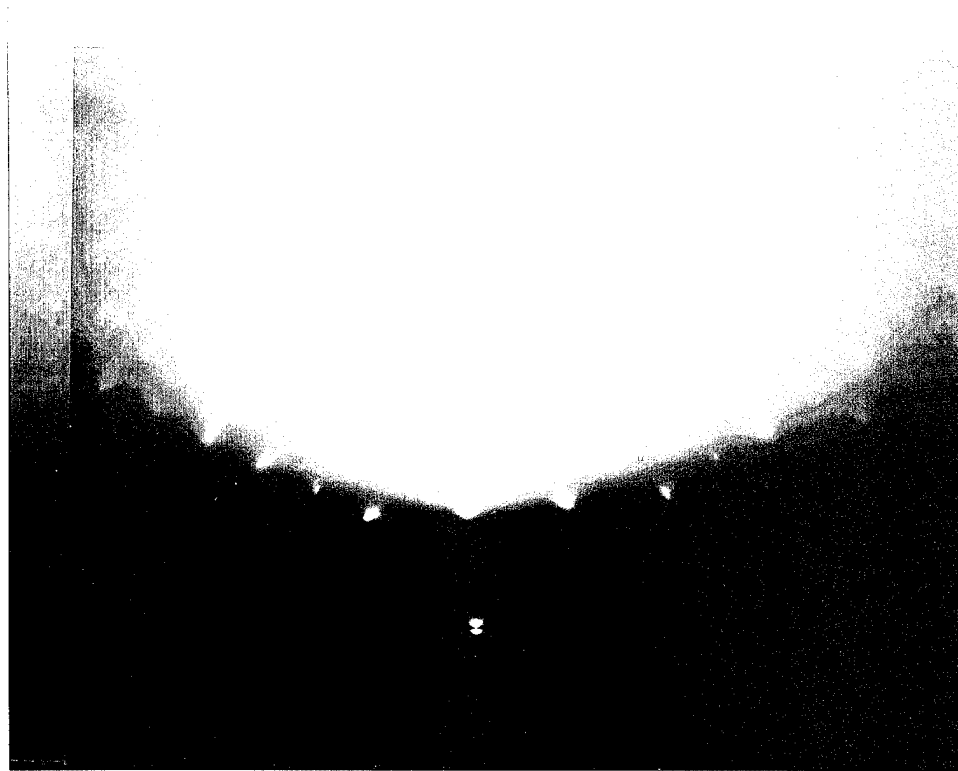


Figure 11. RHEED pattern for $Zn_{0.5}Ge_{0.5}N$ grown at 650° , showing single crystal habitat.

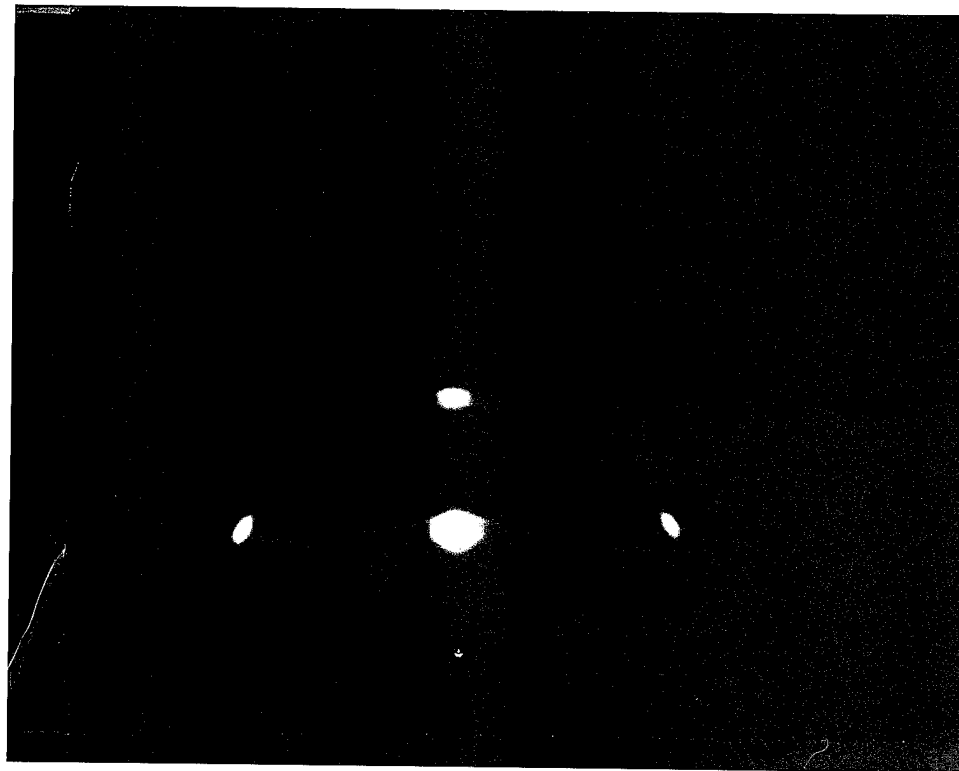


Figure 12. RHEED pattern for single crystal $Zn_{0.5}Ge_{0.5}N$ on GaN.

6.5 Optical Transmission Measurements

A standard Bausch & Lomb monochromator was set up for use in the measurement of the optical transmission of our films. A sketch of the measurement system is shown in Figure 13. Basically, the system was calibrated by measuring the light detected after passage through a sapphire substrate. The calibration therefore takes account of the varying intensity of the incandescent light in the monochromator, and for losses due to reflections

All significant results were obtained from sample 291, which also had the best x-ray diffraction pattern. The transmission pattern of 291 showed a definite cut-off. Many other films just linearly lost transmission throughout the visible portion of the spectrum, which may indicate some amorphous material. Light was passed through a 1 mm iris before impinging on the $Zn_{0.5}Ge_{0.5}N$ film to insure measurement over a uniform portion of the film. A complete set of transmission data, which includes the calculation of the absorption constant, is presented in Table 5. The data have been corrected for a very low level of stray white light through the monochromator, which only affects the data at wavelengths below 350 nm. We take the form of the transmission characteristic as:

$$T = \frac{I}{I_0} e^{-\alpha d} \quad (1)$$

where α is the absorption constant and d is the thickness of the specimen. Determination of d is discussed below. A typical transmission characteristic for single crystal $Zn_{0.5}Ge_{0.5}N$ is shown in Figure 14.

When a material has a direct bandgap, then the relationship between the absorption constant α and the energy E of the light is given by,

$$\alpha = A(E - E_G)^{\frac{1}{2}} \quad (2)$$

where E_G is the bandgap. A plot of α^2 vs E should yield a straight line, and the intercept of this line with the E -axis is the bandgap. Figure 15 is such a plot for $Zn_{0.5}Ge_{0.5}N$. Most of the data points indeed fall on a straight line, which indicates that the material has a direct bandgap. The intercept is at 2.8 eV. Thus the band edge is at 440 nm, in the deep blue portion of the spectrum.

The film thickness was determined by observing the fringe pattern in an optical microscope. The film did not have a uniform thickness, and one area of the substrate was free of any film. Thus we could observe first order fringes starting from the region with no film. Assuming that the refractive index of $Zn_{0.5}Ge_{0.5}N$ is the same as GaN, 2.4, then we calculate that the region of the film where the transmission was measured, which appears as a green fringe, is 110 nm thick. A photograph of the sample showing the fringes is given in Figure 16.

Table 5
Optical Transmission Measurements on $Zn_{0.5}Ge_{0.5}N$ Film

MATERIAL:	ZnGeN2						SUBSTRATE	Sapphire					
	DATE:	1/24/96	1 mm	Output slit:		1 mm		Aperture	1.0 mm				
Wavelength	Amplifier	Gain	Sample Signal, V	Correct for stray light	X1000	Substrate Signal, V	Correct for stray light	Samp/sub Ratio	Normalize (.71844492)	2.3025* Log(I/I0)	Absorb. Const., /cm	Energy, eV	alpha squared
10^x													
330	7	0.0338	0	0	0.045	0	ERR	ERR	ERR	ERR	150185.972	3.757576	
340	7	0.0339	0.0001	0.0001	0.045	0	ERR	ERR	ERR	ERR	153002.956	3.647059	
350	7	0.0341	0.0003	0.0003	0.045	0	ERR	ERR	ERR	ERR	156639.586	3.542857	
355	7	0.0342	0.0004	0.0004	0.0475	0.0025	0.16	0.2227032241	1.50185972	1.50185.972	3.492958	2.26E+10	
360	7	0.0345	0.0007	0.0007	0.0495	0.0045	0.15555556	0.2165170234	1.53002956	1.53002.956	3.444444	2.34E+10	
365	7	0.0359	0.0021	0.0021	0.059	0.014	0.15	0.2087842726	1.566359586	1.56639.586	3.39726	2.45E+10	
370	7	0.04104	0.00724	0.00724	0.0885	0.0435	0.16643678	0.2316625492	1.46241945	1.46241.945	3.351351	2.14E+10	
375	7	0.0497	0.0159	0.0159	0.139	0.094	0.16914894	0.235437584	1.44625599	1.44625.599	3.306667	2.09E+10	
380	7	0.0626	0.0288	0.0288	0.203	0.158	0.18227848	0.2537125337	1.37150272	1.37150.272	3.263158	1.88E+10	
385	7	0.0803	0.0465	0.0465	0.289	0.244	0.19057377	0.2652587069	1.32700063	1.32700.063	3.220779	1.76E+10	
390	7	0.1033	0.0695	0.0695	0.385	0.34	0.20441176	0.284519744	1.25690618	1.25690.618	3.179487	1.58E+10	
395	7	0.13	0.0962	0.0962	0.488	0.443	0.21715576	0.302258044	1.19642.995	1.19642.995	3.139241	1.43E+10	
400	7	0.16	0.1262	0.1262	0.586	0.541	0.23327172	0.324689745	1.12484352	1.12484.352	3.1	1.27E+10	
405	7	0.195	0.1612	0.1612	0.695	0.65	0.248	0.345189973	1.06362099	1.06362.099	3.061728	1.13E+10	
410	7	0.242	0.2082	0.2082	0.8	0.755	0.27576159	0.383831219	0.95751697	0.95751.697	3.02439	9.17E+09	
415	7	0.292	0.2582	0.2582	0.92	0.875	0.29508571	0.4107283747	0.88979029	0.88979.0288	2.987952	7.92E+09	
420	7	0.347	0.3132	0.3132	1.056	1.011	0.30979228	0.4311983789	0.84115593	0.84115.5932	2.952381	7.08E+09	
425	7	0.41	0.3762	0.3762	1.185	1.14	0.33	0.4593253996	0.77796764	0.77796.7637	2.917647	6.05E+09	
430	7	0.483	0.4492	0.4492	1.33	1.285	0.34957198	0.4865675499	0.72035292	0.72035.2916	2.883721	5.19E+09	
435	4	0.000562	0.000528	0.528	1.48	1.435	0.36794425	0.5121398184	0.66913288	0.66913.2879	2.850575	4.48E+09	
440	4	0.000656	0.000622	0.622	1.63	1.585	0.39242902	0.5462200527	0.60471101	0.60471.1009	2.818182	3.66E+09	
445	4	0.00076	0.000726	0.726	1.81	1.765	0.41133144	0.5725302432	0.55766911	0.5576691.109	2.786517	3.11E+09	
450	4	0.000877	0.000843	0.843	2	1.955	0.43120205	0.6001880367	0.51049341	0.51049.3412	2.755556	2.61E+09	
455	4	0.00101	0.000976	0.976	2.21	2.165	0.45080831	0.6274779062	0.46602959	0.46602.9595	2.725275	2.17E+09	
460	4	0.00113	0.001096	1.096	2.39	2.345	0.4673774	0.6505403347	0.42993609	0.42993.6088	2.695652	1.85E+09	
465	4	0.00127	0.001236	1.236	2.59	2.545	0.48565815	0.679582283	0.39156958	0.391569584	2.666667	1.53E+09	
470	4	0.00142	0.001386	1.386	2.82	2.775	0.49945946	0.6951951995	0.36354917	0.36354.9175	2.638298	1.32E+09	
475	4	0.00156	0.001526	1.526	3.04	2.995	0.50951586	0.7091926543	0.343615364	0.34361.5364	2.610526	1.18E+09	
480	4	0.00176	0.001726	1.726	3.23	3.185	0.541915273	0.7542891773	0.28196904	0.28196.904	2.583333	7.95E+08	
485	4	0.00191	0.001876	1.876	3.51	3.465	0.54141414	0.7535917178	0.28289409	0.28289.4091	2.556701	8E+08	
490	4	0.002135	0.002101	2.101	3.79	3.745	0.56101469	0.7808736211	0.24733282	0.24733.2818	2.530612	6.12E+08	
495	4	0.0023	0.002266	2.266	4.06	4.015	0.56438356	0.7855627424	0.24134603	0.24134.6029	2.505051	5.82E+08	
500	4	0.00245	0.002416	2.416	4.31	4.265	0.56647128	0.7884686245	0.23765338	0.23765.3882	2.48	5.65E+08	
505	4	0.00269	0.002656	2.656	4.59	4.545	0.58437844	0.8133935137	0.20653263	0.20653.2627	2.455446	4.27E+08	
510	4	0.00282	0.002786	2.786	4.88	4.835	0.5762151	0.8020310008	0.22059986	0.22059.9865	2.431373	4.87E+08	
515	4	0.00314	0.003106	3.106	5.19	5.145	0.60369291	0.840277278	0.17401698	0.17401.6977	2.407767	3.03E+08	
520	4	0.00326	0.003226	3.226	5.43	5.385	0.59907149	0.8338447085	0.18170138	0.18170.138	2.384615	3.3E+08	
525	4	0.00358	0.003546	3.546	5.73	5.685	0.6237467	0.8681900094	0.14133946	0.14133.946	2.361905	2E+08	
530	4	0.00375	0.003716	3.716	6.02	5.975	0.62192469	0.8656539546	0.14426471	0.14426.4709	2.339623	2.08E+08	
535	4	0.00405	0.004016	4.016	6.33	6.285	0.6389817	0.8893955329	0.11720889	0.11720.8892	2.317757	1.37E+08	
540	4	0.00428	0.004246	4.246	6.61	6.565	0.64676314	0.9002264751	0.10510502	0.10510.5024	2.296296	1.1E+08	
545	4	0.00453	0.004496	4.496	6.89	6.845	0.6568298	0.9142382171	0.0896608	0.08966.07965	2.275229	80390584	
550	4	0.00475	0.004716	4.716	7.22	7.175	0.65728223	0.9148679484	0.08897225	0.08897.22547	2.254545	79160521	
555	4	0.00498	0.004946	4.946	7.51	7.465	0.66255861	0.9222121117	0.08097703	0.08097.70331	2.234234	65572799	
560	4	0.0052	0.005166	5.166	7.78	7.735	0.6678733	0.9296096118	0.07298786	0.07298.78558	2.214286	53272271	
565	4	0.00504	0.005366	5.366	8.04	7.995	0.67116948	0.9341975456	0.06806484	0.06806.48427	2.19469	46328228	
570	4	0.00565	0.005616	5.616	8.33	8.285	0.67785154	0.9434982697	0.0581586	0.05815.8987	2.175439	35824226	
575	4	0.00584	0.005806	5.806	8.57	8.525	0.68105572	0.9479581517	0.05344295	0.05344.29464	2.156522	28561485	
580	4	0.00602	0.005986	5.986	8.82	8.775	0.68216524	0.9495024924	0.05181521	0.05181.52089	2.137931	26848159	
585	4	0.00621	0.006176	6.176	9.06	9.015	0.68508042	0.9535601614	0.04755105	0.04755.10505	2.119658	22611024	
590	4	0.00639	0.006356	6.356	9.3	9.255	0.68676391	0.9559033578	0.04509679	0.04509.67946	2.101695	20337209	
595	4	0.00656	0.006526	6.526	9.49	9.445	0.69094759	0.9617266016	0.03902362	0.03902.36245	2.084034	15228433	
600	4	0.00672	0.006686	6.686	9.7	9.655	0.69249094	0.9638747774	0.03679253	0.03679.2532	2.066667	13536904	
605	4	0.00687	0.006836	6.836	9.85	9.805	0.69719531	0.9704227688	0.03002235	0.03002.3488	2.049587	9013414	
610	4	0.00701	0.006976	6.976	10.06	10.015	0.69655517	0.9695317593	0.03049049	0.03049.09029	2.032787	9573395	
615	4	0.00718	0.007146	7.146	10.23	10.185	0.70162003	0.9765815164	0.02369618	0.02369.61782	2.01626	5615089	
620	4	0.00725	0.007216	7.216	10.4	10.355	0.69686142	0.9699580305	0.03050135	0.03050.13487	2	9303323	
625	4	0.00739	0.007356	7.356	10.55	10.505	0.70023798	0.9746578512	0.02566784	0.02566.78428	1.984	6588382	
630	4	0.00748	0.007446	7.446	10.74	10.695	0.69521318	0.9805055754	0.03143197	0.03143.19694	1.968254	9879687	
635	4	0.00765	0.007616	7.616	10.86	10.815	0.70420712	0.9801824749	0.02001579	0.02001.57861	1.952756	4006317	
640	4	0.00771	0.007676	7.676	10.94	10.895	0.70454337	0.9806504979	0.019535843	0.01953.84321	1.9375	3817503	
645	4	0.00783	0.007795	7.795	11.08	11.035	0.70647938	0.9833452282	0.0167944	0.01679.44013	1.922481	2820519	
650	4	0.00785	0.007816	7.815	11.2	11.155	0.70067234	0.975264238	0.02504775	0.02504.77514	1.907692	6273898	
655	4	0.00798	0.007946	7.945	11.3	1							

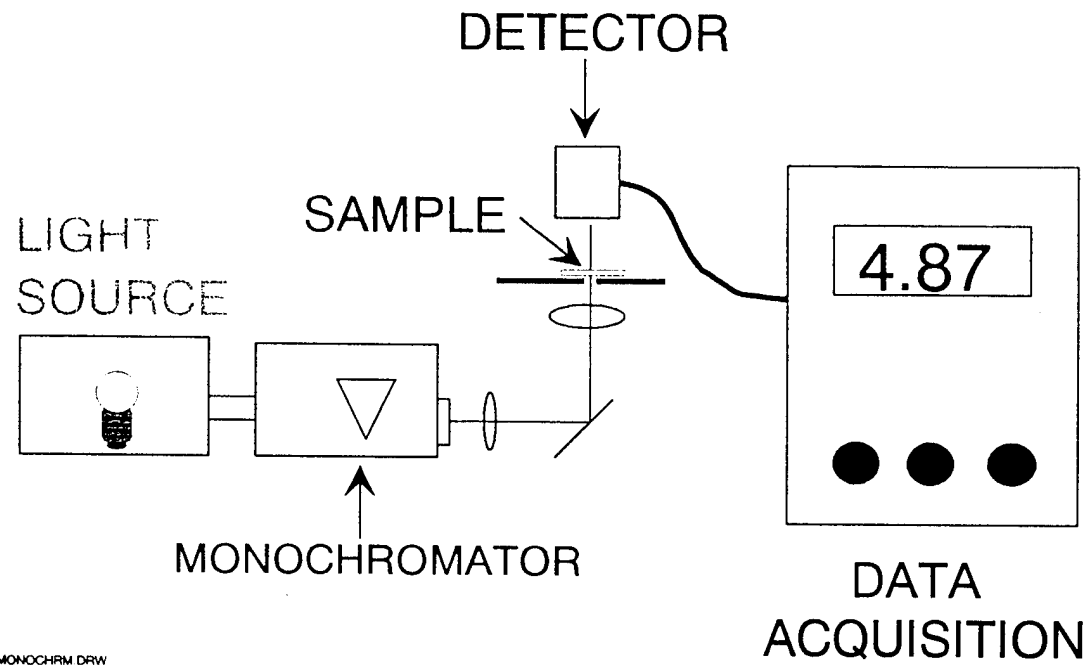


Figure 13 *Diagram of our optical transmission measurement system*

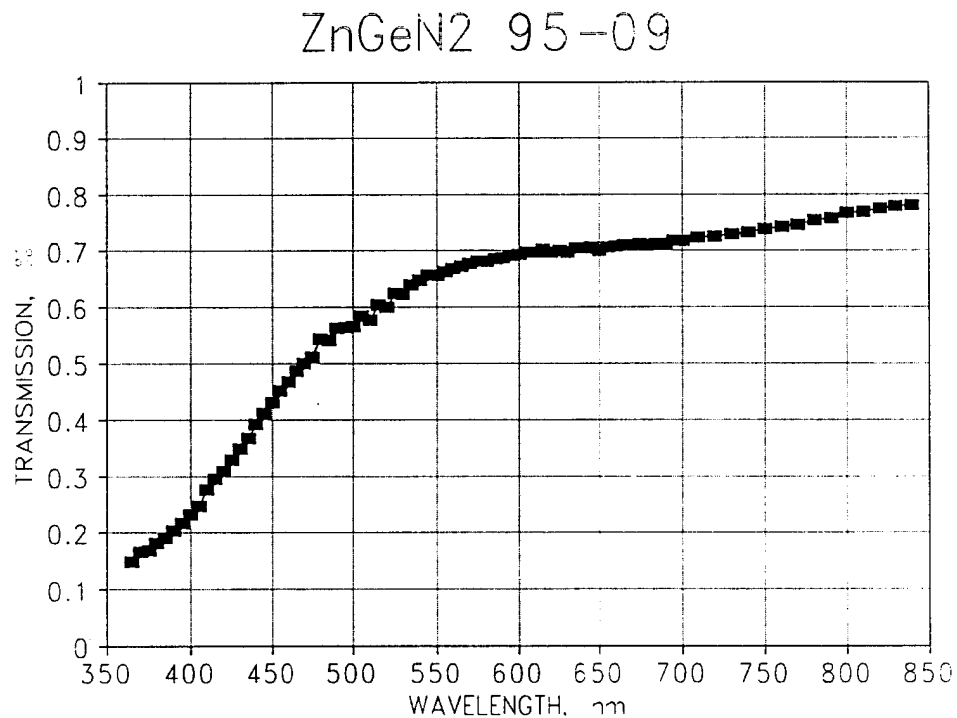


Figure 14 *Transmission characteristic for single crystal Zn_{0.5}Ge_{0.5}N*

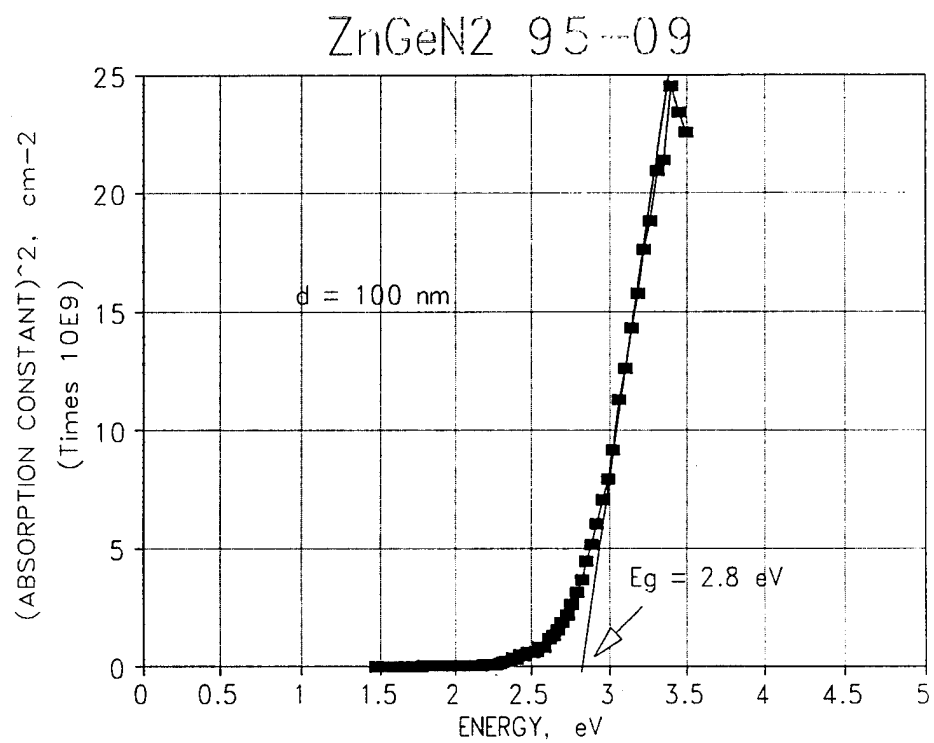


Figure 15 Determination of the bandgap of $\text{Zn}_{0.5}\text{Ge}_{0.5}\text{N}$



Figure 16 Fringe pattern for $\text{Zn}_{0.5}\text{Ge}_{0.5}\text{N}$ film

6.6 Electrical Conductivity of $Zn_{0.5}Ge_{0.5}N$

Sample 291 was cleaved to form a rectangular bar 5 mm long and 2 mm wide. Indium contact dots were affixed to each end of the bar. A current-voltage characteristic was obtained with a Tektronix 577 curve tracer. The characteristic proved to be a straight line, indicating good ohmic contacts. With 20 volts of either polarity applied to the bar, a current of 12 mA flowed. The resistance was calculated from $R = V/I$, which gave $1.67 \times 10^6 \Omega$. The resistivity was obtained from,

$$\rho = R \frac{A}{L} \quad (3)$$

where A = cross section area and L = length. We find that $\rho = 6.7 \Omega\text{-cm}$.

It was not possible to determine the conductivity type by using a thermoelectric probe, probably because the film is so thin. It was not possible to make a Hall effect measurement. However, if we assume that the mobility is $10 \text{ cm}^2/\text{V}\text{-s}$, then the carrier concentration would be about 10^{17} cm^{-3} . This is a very comfortable result.

7 PLANS FOR PHASE II

The Phase I results have been quite exciting. NZ Applied Technologies has concluded that the devices which would be of greatest interest to the commercial sector are blue diode lasers based on $Zn_{0.5}Ge_{0.5}N$. We suggest that blue lasers will also be of great interest to the Air Force for secure communications linked and for increased data storage on aircraft and spacecraft. Therefore, in Phase II, we shall propose to concentrate on demonstrating high intensity junction diodes followed by injection lasers fabricated with our new $Zn_{0.5}Ge_{0.5}N$ material.

In Phase II, we shall continue to vary the growth conditions to improve our control over the properties of our $Zn_{0.5}Ge_{0.5}N$ films. We have just finished a major rebuilding of our deposition system, and we now can use a much improved reaction chamber for growing $Zn_{0.5}Ge_{0.5}N$. The new chamber can make use of Nakamura's "two flow growth" technique, whereby the reactants are supplied parallel to the substrate surface, with a second high capacity vertical flow of carrier gas to hold the reactants near the substrate surface through momentum transfer. The new reactor can operate at temperatures as high as 1000°C , and has ammonia gas available as the group V source. We expect to obtain even better results in Phase II efforts in our improved reactor.

We shall continue to deposit single crystal films of $Zn_{0.5}Ge_{0.5}N$ on GaN, and we shall study the interface between GaN and $Zn_{0.5}Ge_{0.5}N$ in close detail using high resolution transmission electron microscopy. We are going to continue our all of our characterization work, including instituting an electron diffraction study to see if Zn-Ge ordering on the lattice can be identified. Measurements of photoluminescence will be a high priority, because typically, unless a sample exhibits photoluminescence, it is unlikely that it can produce electroluminescence.

Control of doping will be very important. We must determine if both n- and p-type

doping can be demonstrated just by varying the growth conditions, as has been shown for $Zn_{0.5}Ge_{0.5}P$. Otherwise, extrinsic dopants must be identified. It may prove possible to form single phase alloys with GaN by admitting a gallium precursor during film growth. This approach could provide a fourth adjustable parameter for control of doping.

Junction diodes will be formed, and device characteristics will be monitored. Electroluminescence will be closely studied. Once simple diodes have been formed, laser structures can be fabricated. To form an edge emitting laser, we shall provide optical confinement with GaN or AlGaN cladding layers, as required. Heterojunctions between $Zn_{0.5}Ge_{0.5}N$ and GaN will also be investigated. In addition to the use of these heterojunctions as light emitting devices, they will also give pertinent information for future work with $Zn_{0.5}Ge_{0.5}N$ transistors.

8 BACKGROUND INFORMATION

8.1 Heterojunction Transistors

For very high speed and high gain operation, it has proven advantageous to develop transistors containing *heterojunctions*.³¹ The basic principle governing the operation of a heterojunction transistor is that either the base or the channel is surrounded by regions of higher band gap. This potential energy step prevents the leakage of minority carriers from the base into the emitter, or guides the introduction of charges from the spacer into the undoped channel. The HBT emitter injection efficiency is improved without needing to resort to ultra-high doping levels in the emitter, improving both the gain and the bandwidth. However, a bipolar transistor is a low-field minority carrier device, and it therefore requires low defect density epitaxial material to function successfully. Therefore, it would be useful to find a material which is closely lattice matched to GaN, but which offers a smaller bandgap, to function as the base of a nitride HBT. The high speed performance of a MODFET relies on the introduction of charges from a doped spacer across a potential barrier into the undoped, high mobility channel. In contrast to the bipolar case, field effect transistors are majority carrier devices that can be made with a material that only affords one type of mobile carrier. Once again, though, crystal defects in the channel due to lattice mismatching will deteriorate the carrier mobility and compromise the performance of a MODFET, leading to the desire for a lattice-matched smaller bandgap partner for GaN.

The III-V semiconductors are receiving the most attention for heterojunction transistor research. Common emitter unity current gain has been achieved at frequencies as high as 105 GHz for $Al_xGa_{1-x}As/GaAs$ HBTs, where the $Al_xGa_{1-x}As$ material provides the wide band gap emitter.³² MODFETs have been reported with unity current gain at frequencies as high as 113 GHz,³³ and transconductances approaching 600 mS/mm.³⁴ However, none of these materials systems is capable of being used at high temperatures; in fact, life-testing of AlGaAs/GaAs MODFETs indicated a mean time to failure of only about 20 hours at 300°C.³⁵ We propose that HBTs fabricated from $Zn_{0.5}Ge_{0.5}N/GaN$ will fulfill the pressing need for transistors which have large gain-bandwidth products and operate at high temperatures. Such devices will find service both for the Air Force, and for a variety of commercial customers.

8.2 GaN Transistors

The principle reason for an interest in the wide band gap nitride semiconductors is their potential use in high power, high temperature, high frequency microelectronic devices which are also resistant to radiation damage. There special needs for semiconductor devices that can continue to operate in high temperature, hostile environments. Applications for high operating temperature transistors can be found in avionics (engine control) and for nuclear and conventional power plants. In any of these applications, it is advantageous to perform some processing of sensor and control data in situ, to lessen data corruption over long transmission lines. Because a GaN/ $Zn_{0.5}Ge_{0.5}N$ transistor features very wide band gap materials, it will be able to operate without a problem in high temperature applications.

GaN is the basic material for band gap engineered structures which exhibit absorption and emission edges throughout the visible spectrum and the near ultraviolet. Developments on using MOCVD to deposit GaN, AlN and their alloys have been reported by several research teams; a recent review of GaN technology has been given by Davis.³⁶ Recently, Norris *et al.*, have succeeded in preparing high conductivity p-type samples of GaN doped with Mg in NZ Applied Technologies' PE-MOCVD reactor.²⁹ Therefore, GaN film growth is quite advanced, and the material can be used to form the emitter and collector for a pnp transistor, with an n-type $Zn_{0.5}Ge_{0.5}N$ base.

Asif Khan and co-workers have recently announced the first demonstration of a GaN metal semiconductor field effect transistor (MESFET).^{37,38} They deposited 600 nm of unintentionally doped n-type GaN on an AlN buffer layer using a (0001) sapphire substrate. The n-type GaN formed the conducting channel for this MESFET. With a carrier concentration of $1 \times 10^{17} \text{ cm}^{-3}$, the channel was completely depleted at a reverse bias of -12V on the gate. The measured transconductance was about 20 mS/mm. This group has now also produced a MODFET based on a two dimensional electron gas situated at a GaN-Al_xGa_{1-x}N heterojunction.³⁹ Once again using a sapphire substrate overcoated with an AlN buffer layer, they deposited a 600 nm n-type GaN channel with a 100 nm n-type Al_{0.14}Ga_{0.86}N cap layer. The transconductance of this device was measured to be 28 mS/mm. The low transconductance may be attributed to the high level of background doping in the nitride layers, which is at the $1 \times 10^{18} \text{ cm}^{-3}$ level.⁴⁰ However, the results clearly show the feasibility of producing FETs based on GaN.

9 REFERENCES

1. K. Shenai, R. S. Scott, B. J. Baliga, *IEEE Trans. Electron. Dev.*, **36**, 1811 (1989).
2. S. Yoshida, S. Misawa, S. Gonda, *J. Appl. Phys.*, **53**, 6844 (1982).
3. "Plasma Assisted Deposition of In_xGa_{1-x}N Films for High Temperature Heterostructure Transistors," with Yi-Kang Pu and E. A. Johnson, *2nd International High Temperature Electronics Conf.*, Charlotte, P225, June 5-10, 1994.
4. T. Matsuoka, N. Yoshimoto, T. Sasaki, A. Katsui, *J. Electronic Materials*, **21**, 157 (1992).

5. Shuji Nakamura, presented at the Fall Materials Research Society Conference, Session AAA, Nov. 27-Dec. 1, 1995.
6. Shuji Nakamura, Takashi Mukai, Masayuki Senoh, "Candela-class high brightness InGaN/AlGaN double heterostructure blue light-emitting diode," *Appl. Phys. Lett.*, 64, 1687 (1994).
7. Shuji Nakamura, Masayuki Senoh, Shinichi Nagahama, Naruhito Iwasa, Takao Yamada, Toshio Matsushita, Hiroyuki Kiyoku, Yasunobu Sugimoto, *Japan. J. Appl. Physics*, 35, L74 (January 15, 1996).
8. N. Nakayama *et al*, *Electronics Letter*, 30, 568 (1994).
9. M. Asif Khan et al, "Metal-semiconductor FET with GaN" *Appl. Phys. Lett.* 62, 1786 (Apr 1993).
10. M. Asif Khan et al, "HEMT based on GaN-AlGaN" *Appl. Phys. Lett.* 63, 1214 (Aug 1993).
11. M. Asif Khan et al, "Schottky Barrier Photodetector with Mg-doped GaN" *Appl. Phys. Lett.* 63, 2455 (Nov 1993).
12. Warren Johnson, James Parsons, M.C. Crews, "Nitrogen Compounds of Gallium" *Journal of Physical Chemistry* 36 2651 (1932)
13. Robert Juza, Harry Hahn, "Uber die Kristallstrukturen von Cu₃N, GaN und InN" *Zeitschrift fur anorganische und allgemeine Chemie* 239 282 (1938)
14. H.P. Maruska, J.J. Tietjen, "The Preparation and Properties of Vapor-Deposited Single-Crystalline GaN" *Appl. Phys. Lett.* 15 327 (1969)
15. H.P. Maruska D.A. Stevenson, J.I Pankove "Violet Luminescence of Mg-doped GaN" *Appl. Phys. Lett.* 22 (1973).
16. H. P. Maruska and D. A. Stevenson, "Mechanism of light production in metal-insulator-semiconductor diodes: gallium nitride (magnesium) light-emitting diodes," *Solid State Electronics*, 17, 1171 (1974).
17. H.M. Manasevit, F.M. Erdmann, W.I. Simpson "The Use of Metalorganics in the Preparation of Semiconductor Materials" *J. Electrochem. Soc.* 118 (1971)
18. See, for example, J. H. Edgar, *J. Mater. Res.*, 7, 235 (1992).
19. H.P. Maruska, W.C. Rhines, D.A. Stevenson, " Preparation of Mg-Doped GaN Diodes Exhibiting Violet Eletroluminescence" *Mat. Res. Bull.* 7 777 (1972)
20. S. Nakamura et al, "P-type Mg-doped GaN," *Jpn J. Appl. Phys.* 30, L1708 (Oct 1991).

21. William L. Larson, H. Paul Maruska, David A. Stevenson, "Synthesis and Properties of ZnGeN₂," *J. Electrochem. Soc.*, 121, 1673 (Dec. 1974).
22. M. Maunaye and J. Lang, *Mat. Res. Bull.*, 5, 793 (1970).
23. T. Endo *et al*, *J. Mat. Sci. Lett.*, 11, 424 (1992).
24. F. F. Grekov et al, *Inorganic Materials*, 15, 1546 (1979).
25. M. Wintenberger, *Mat. Res. Bull.*, 8, 1049 (1973).
26. G. D. Boyd, E. Buehler, F. G. Storz, *Appl. Phys. Lett.*, 18, 301 (1971).
27. David F. Bliss, Meckie Harris, Jane Horrigan, William M. Higgins, Alton F. Armington, Joseph A. Adamski, *J. Crystal Growth*, 137, 145 (1994).
28. G. C. Xing, K. J. Bachmann, J. B. Posthill, M. L. Timmons, *Mat. Res. Soc. Symp. Proc.*, 162, 615 (1990).
29. L. D. Zhu, P. E. Norris, J. Zhao, Proc. International Conf. on Compound Semiconductors, San Diego, CA, Sept. 1994.
30. G. C. Xing *et al*, *J. Crystal Growth*, 94, 381 (1989).
31. Fazal Ali and Aditya Gupta, HEMTs and HBTs: Devices, Fabrication, and Circuits, Artech House, Boston, 1991.
32. T. Ishibashi *et al*, IEDM Tech. Dig., 1988, pp. 826-829.
33. A. N. Lepore *et al*, *Electron. Lett.*, 24, 364 (1988).
34. A.M. Kusters, A. Kohl, R. Muller, V. Sommer, K. Heime, *IEEE Electron Device Lett.*, 14, 36 (1993).
35. P. C. Chao, A. Swanson, A. Brown, U. Mishra, F. Ali, C. Yuen, Chapter 3 in HBTs and HEMTs, Ali and Gupta, eds., Artech House, Boston, 1991, page 189.
36. R.F. Davis, *et al*, *Mat. Sci. and Engr.* B1 77 (1988).
37. M. Asif Khan *et al*, *Appl. Phys. Lett.*, 60, 3792 (1992).
38. M. Asif Khan *et al*, *Appl. Phys. Lett.*, 62, 1786 (1993).
39. M. Asif Khan *et al*, *Appl. Phys. Lett.*, 63, 1214 (1993).
40. M. Asif Khan *et al*, *Appl. Phys. Lett.*, 60, 3027 (1992).